Construction and Building Materials 426 (2024) 136075

Contents lists available at ScienceDirect

Construction and Building Materials

journal homepage: www.elsevier.com/locate/conbuildmat

A machine-learning based approach to estimate acoustic macroscopic parameters of porous concrete

Luís Pereira *, Luís Godinho, Fernando G. Branco, Paulo da Venda Oliveira

University of Coimbra, ISISE, ARISE, Department of Civil Engineering, Coimbra, Portugal

ARTICLE INFO

Keywords:
Porous concrete
Artificial neural networks, Macroscopic Parameters
Sound absorption coefficient

ABSTRACT

Porous concrete with expanded clay inherent porosity makes it an interesting and effective acoustic material, applied in numerous scenarios such as highways, airports and architectural structures, due to its capacity to mitigate noise pollution, by absorbing and damping sound waves. It is usually accepted that macroscopic properties such as open porosity, tortuosity or airflow resistivity of such materials play a fundamental role in the definition of the internal absorption process. This study explores the application of tailored artificial neural networks (ANNs) for predicting first the macroscopic properties (open porosity, tortuosity and airflow resistivity) and then the sound absorption coefficient (α) of these porous concrete mixtures, using only two input parameters (size class of the expanded clay and density of the test specimens). The results demonstrate the efficacy of the proposed ANN approach in accurately predicting macroscopic properties and the sound absorption coefficient of these mixtures, making it possible to obtain such important parameters in an effective and much simpler way.

1. Introduction

Porous concrete, especially when formulated with expanded clay aggregates, has emerged as a versatile material with increasing applications in various construction scenarios, with numerous applications, from flooring where rapid drainage into the underlying soil is desired, to thermal insulation especially in areas with cold climates, to acoustic insulation in communication routes, and also in industrial settings, among others [1]. Originally appreciated for its lightweight and eco-friendly attributes, porous concrete has evolved to play a crucial role in noise control and acoustic engineering, both indoors and outdoors [2]. These materials exhibit high values of sound absorption due to its unique structure, where the assembly of irregular shaped porous grains result in a network of air-filled channels. This unique composition facilitates effective sound absorption by promoting multiple interactions of sound waves within the material, dissipating and attenuating them effectively [3,4]. Additionally, these materials prepared with expanded clay exhibit acceptable mechanical characteristics and the ability to withstand atmospheric conditions over long periods of time, also contributing to the reduction of the dead load of structures and are considered cheap and easy-to-apply alternatives to other types of porous concrete [5,6].

Understanding the acoustic behaviour of porous concrete requires the characterization of parameters such as porosity, tortuosity, and airflow resistivity. These parameters can be determined directly or by means of use of theoretical models such as the Horoshenkov-Swift method, among others. The direct determination is not always easy due to specific properties of the material, such as low density and closed unconnected pores, and demands the preparation and laboratory testing of specimens, with the inherent investment of time and financial resources. The inverse methodologies require the prior assessment of the surface impedance and the absorption coefficient [7].

While these traditional methods have proven valuable, the advent of artificial neural networks (ANNs) introduces a more comprehensive approach to determining these parameters. ANNs overcome in capturing complex relationships within datasets, offering improved accuracy in predicting parameters such as porosity, tortuosity, and airflow resistivity. Their ability to generalize from training data to predict parameters for unseen cases enhances their applicability in optimizing porous concrete formulations for specific acoustic requirements [8].

The purpose of this work is to assess the possibility of using artificial neural network models to accurately predict three non-acoustic (output) parameters of paramount importance to characterize porous concrete (open porosity, tortuosity and airflow resistivity) using only two (input)

* Corresponding author.
E-mail addresses: lfmpereira@student.uc.pt (L. Pereira), lgodinho@dec.uc.pt (L. Godinho), fjbranco@dec.uc.pt (F.G. Branco), pjvo@dec.uc.pt (P. da Venda Oliveira).

https://doi.org/10.1016/j.conbuildmat.2024.136075
Received 23 January 2024; Received in revised form 7 March 2024; Accepted 28 March 2024
Available online 9 April 2024

Fig. 1. Unbound samples of the size classes of expanded clay used in this study: a) "0–2"; b) "2–4"; and c) "3–8". Adapted from [10].

Fig. 2. Example of test specimens prepared with each of the size classes of expanded clay used in this study.

easily obtained parameters to feed the training of the ANN: the size class of the material and the density of the mixture. The input parameter size class is provided by the manufacturer and the density was physically determined, weighing and measuring the test specimen. In what concerns the output parameters, the open porosity was experimentally obtained, and the tortuosity and airflow resistivity were determined applying an inverse method, which required the experimental data resulting from the impedance tube test [9], the surface impedance and the absorption coefficient [10]. For the purpose of this study a large set of samples produced using different mixtures of porous concrete based on three different aggregate classes has been tested using the impedance tube method, and the corresponding macroscopic parameters were then estimated by inversion (for the case of tortuosity and airflow resistivity) or by direct measurement (for the case of open porosity). An ANN has then been trained using these set of parameters, and considering the input parameters mentioned before (density and size class). The values of the macroscopic parameters predicted by the ANN (open porosity, tortuosity and airflow resistivity) were then used to estimate the absorption coefficient (α) for the frequency range of 125–2000 Hz using the semi-phenomenological proposed by Horoshenkov-Swift [7].

This article is organized with the following structure: (1) *Introduction*, where a condensed presentation of the objectives and pertinence of the research is described, (2) *Materials, specimen preparation and methods used*, where the materials and compositions of the test specimens are explained, (3) *Horoshenkov and Swift methodology* and (4) *Machine Learning*, chapters where the general theory and applications of both methodologies are outlined, (5) *Results and Discussion*, where the outcome of this research is explained and presented, and finally (6) *Conclusions*, the culminating section of the study, with the essential remarks, providing a synthesis of the research findings and their implications.

Table 1
Summary of the mixtures used in this study (adapted from [10]). * - Ratio Aggregate/Cement/Water, in percentage.

Granular mixture	A/C/W* (%)	Commercial designation	Thickness (cm)
Mixture 1	48.48/34.43/17.20	2–4	4
			6
			8
		3–8	4
			6
			8
Mixture 2	43.96/37.36/18.68	0–2	4
			6
			8
		2–4	4
			6
			8
		3–8	4
			6
			8
Mixture 3	40.17/38.89/19.92	0–2	4
			6
			8

2. Materials, specimen preparation and methods used

The materials used in the preparation of the test specimens were tap water, Portland cement type 1 (42.5 R), and three granulometric classes of expanded clay with the commercial designation "0–2", "2–4" and "3–8". Fig. 1 shows the different size classes of expanded clay used in this study.

Fig. 2 presents an example of test specimens prepared with each of the size classes of expanded clay used in this study.

The designation of the mixtures, the ratio aggregate/cement/water content, and the thickness of the test specimens is presented in Table 1 (these test specimens were already used in a different study [10]).

The guidelines indicated in the ISO10534–2:2001 standard were followed to obtain the sound absorption coefficient. The impedance tube used in this laboratory test has a circular cross-section with a diameter of 10.1 cm and the analysed frequency range was 100–1800 Hz. The obtained pressure data was processed using a MATLAB script to calculate both surface impedance and sound absorption coefficient. The open porosity (ϕ) was experimentally determined through the water saturation method, where ϕ is equal to the ratio of the volume fluid-space (V_f) by the volume of the material sample (V_t), as represented in Eq. (1):

$$\phi = V_f / V_t \tag{1}$$

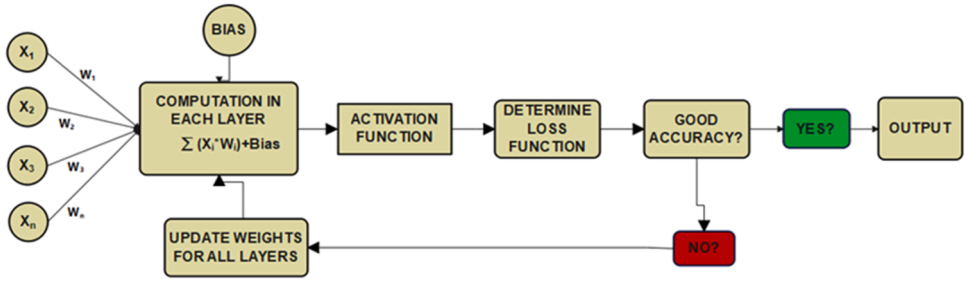

Fig. 3. Diagram illustrating the operation of a supervised neural network with backpropagation. Reprinted from [29].

The volume of the fluid-space is given by (2):

$$V_f = (M_{sat}/M_{dry})/\rho_{water} \tag{2}$$

with M_{sat} being the mass of the sample saturated with water and M_{dry} being the dry sample, and finally the ρ_{water} being the density of the water (which depends on the temperature).

A more detailed description of the procedure adopted in preparing these specimens is shown in the article Pereira et al. [10]. All the remaining parameters were determined applying an inversion methodology based on a genetic algorithm.

3. Horoshenkov and swift methodology

Horoshenkov and Swift developed a theoretical methodology [11] that is capable of accurately predict the acoustic properties of consolidated porous concrete materials, from four non-acoustic parameters, (i) open porosity (ϕ), (ii) tortuosity (α_∞), (iii) standard deviation of the pore size(σ_p), and (iiii) airflow resistivity (σ). In this study, these parameters were obtained using a genetic algorithm to search within physical limits known to be acceptable to this type of material [2,6,12]. The model assumes a scenario where a rigid frame porous sample, possessing a cross-sectional area S_0 is penetrated by uniform pores of diverse cross-sectional areas. These pores are conceptualized as a series of capillary tubes with specific shapes, and their sizes adhere to a unique statistical distribution.

Utilizing the four macroscopic parameters, one can derive the characteristic impedance and wave number of the material, facilitating its representation in equivalent fluid models. It is necessary to define the viscosity correction function ($F(\omega)$) (3):

$$F(\omega) = \frac{1 + a_1\epsilon + a_2\epsilon^2}{1 + b_1\epsilon} \tag{3}$$

with $a_1 = \Theta_1/\Theta_2$, $a_2 = \Theta_1$, and $b_1 = a_1$. Assuming a circular pore geometry, $\Theta_1 = \frac{4}{3}e^{4\xi} - 1$ and $\Theta_2 = \frac{e^{3\xi/2}}{\sqrt{2}}$, with $\xi = (\sigma_p \ln(2))^2$ and the dimensionless parameter $\epsilon = \sqrt{j\omega\rho_0\alpha_\infty/(\sigma\phi)}$.

The material's intrinsic characteristics are expressed through its compressibility (C)(4) and complex density (ρ)(5):

$$C = \frac{\phi}{\gamma P_0}\left(\gamma - \frac{\rho_0(\gamma - 1)}{\rho_0 - j\frac{\sigma\phi}{\omega\alpha_\infty N_{pr}}F(N_{pr}\omega)}\right) \tag{4}$$

$$\rho = \frac{\alpha_\infty}{\phi}\left(\rho_0 - \frac{j\phi\sigma}{\omega\alpha_\infty}F(\omega)\right) \tag{5}$$

where γ is the specific heats ratio, P_0 is the atmospheric pressure and N_{pr} is the Prandtl number.

These parameters are then used to determine the characteristic impedance (6) and the complex wave number (7) applying the following equations:

$$Z_c = \sqrt{\rho/C} \tag{6}$$

$$k = \omega\sqrt{\rho C} \tag{7}$$

As already mentioned, the macroscopic parameters (with the exception of the open porosity) were determined applying an inversion method based on a genetic algorithm, by a process of minimization of the difference between the experimental and theoretical predicted acoustic quantities (in this case, the sound absorption coefficient), within the frequency domain [13,14]. This procedure involves the determination of the loss function (also called objective or cost function), obtained from the summation of the quadratic error between the numerical and experimental values, among the frequency range with *nf* discrete values (8):

$$Loss \quad Function(\omega) = \sum_{i=1}^{nf} \left|\alpha_{num_i} - \alpha_{\exp_i}\right|^2 \tag{8}$$

with α_{num_i} being the absorption coefficient obtained form the Horoshenkov-Swift model and $\alpha_{\exp_i}$ being the absorption coefficient obtained from the impedance tube laboratory test.

4. Machine learning

Machine learning (ML) methodologies can process incomplete or imperfect data and capture non-linear relationships among the variables of a given system [15,16]. The use of ML methods as a forecasting technique has been widely applied in numerous areas of human activity, as an alternative to traditional statistical methods, such as biology [17], atmospheric sciences [18], renewable energies [19], polymer composites [20], industrial applications [21], medicine [22], engineering [23], geology and geotechnics [24], among other areas. ML methods are an extremely useful tool to classify and cluster raw input, applying algorithms for reinforcement learning, helping to make informed decisions, thus allowing the generated adaptable models to be applied in new problems with new data, reducing cost and time, both in academic and business contexts [25–27].

An Artificial Neural Network (ANN) is a mathematical (or computational) model that mimics the structural and functional aspects of biological neural networks. It consists of an interconnected group of artificial neurons and processes information using a computational connectionist perspective, altering its structure based on a set of evolving information throughout the learning/training phase. A neuron is a simple mathematical processing unit that takes one or more inputs and produces one or more outputs. Each input is associated with a weight that defines its relative importance, which is then calculated by the neuron, resulting in an output. This output is modified by an activation function (also referred to as a transfer function) and forwarded to another neuron (in another layer), constructing a feed-forward architecture where data flows from inputs to outputs, known as a multi-layer perceptron [28].

A supervised algorithm utilizes a given set of input and response

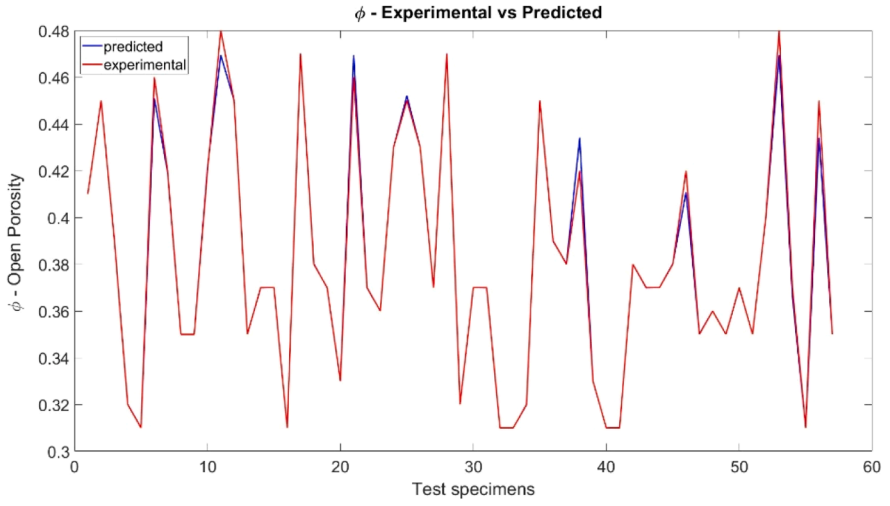

a)

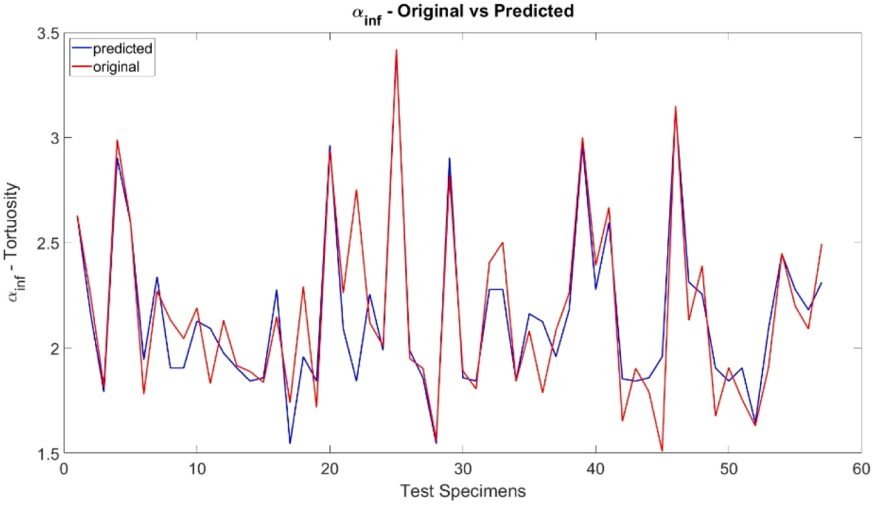

b)

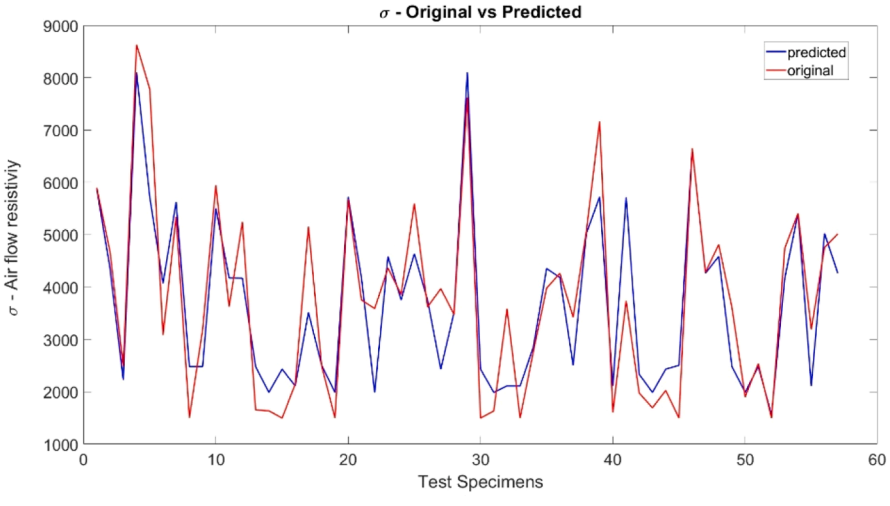

c)

Fig. 4. Overlapping of curves predicted by ANN and obtained by the H-S method. a) open porosity; b) Tortuosity; c) Airflow resistivity.

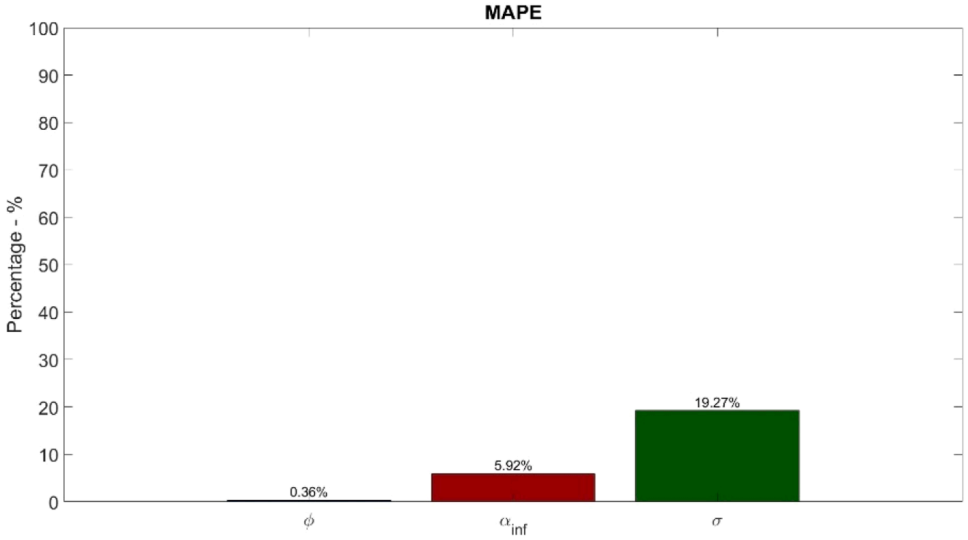

Fig. 5. Mean absolute percentage error for the three output parameters predicted by the ANN model.

parameters to train a model that enables the prediction of these response parameters in the presence of new input parameters. This allows for the comparison of predicted values with actual values, facilitating the improvement of the prediction model's accuracy. Supervised learning methodology employs two techniques to train models: regression and classification. Regression predicts continuous responses, while classification predicts discrete responses by categorizing them [15]. In this study, the regression model was used. Fig. 3 represents a diagram that illustrates the operation of a supervised neural network with backpropagation.

This methodology can be employed to facilitate crucial human activities, such as in non-destructive testing for monitoring the condition of already constructed and in-use structures. It plays a role in the identification and evaluation of pathologies, assessing the risk of landslides, and monitoring the development pace of cracks through acoustic emissions [30–32]. Additionally, it aids in predicting mechanical and physical parameters [33–35], by either reducing or completely replacing laboratory or field tests. Its application extends to predicting macroscopic parameters of granular materials, such as porosity [36], tortuosity, and permeability through image analysis [37,38], ultrasonic propagation [39], or sound absorption coefficient [40].

In this study, several architectures of an ANN were tested, with different number of layers and neurons per layer, different training algorithms (e. g. *trainlm*, *trainscg*, and finally *trainbr*), and also with different activation functions (e. g. *tansig*, *softmax* and *logsig*) and learning rates (e. g. 0.1, 0.01, 0.001). The final configuration of the network comprised five layers with each layer hosting ten neurons. The training algorithm that returned better results was the *trainbr*, recognized for its Bayesian regularization approach, enhancing generalization and with good performance in what concerns the mitigation of overfitting, thus contributing to improved model performance on this study database. In each layer, it was decided to apply the logistic sigmoid (*logsig*) transfer function, a non-linear activation function known for its ability to model intricate relationships in the data. By mapping input values to a range between 0 and 1, the *logsig* function introduces non-linearity, enhancing the neural network's capability to capture complex patterns and dependencies within the input data. The learning rate of 0.01 was the one that returned better results, indicating a gradual convergence of the model, preventing the ANN (1) to settling prematurely into suboptimal solutions (local minimum), and (2) to overshoot, which happens when the adjustment of the weights is excessively large, going beyond the absolute minimum. The database used to train the ANN model was composed initially by 88 test specimens, but the application of a MATLAB function to identify and remove outliers reduce the database to its final size of 82 test specimens. This data set was then randomly divided into training, testing and validation subsets with 70% of the dataset being allocated to the training subset, and 15% being allocated to each of the remaining subsets. This percentage ratio is frequently applied in similar researches [41,42].

5. Results and discussion

The prediction of the three macroscopic parameters (open porosity, tortuosity and the airflow resistivity) obtained by the artificial neural network model (ANN) and the comparison with the same parameters obtained by the inverse algorithm based on the Horoshenkov-Swift (H-S) semi-phenomenological methodology are presented below.

5.1. Determination of the macroscopic parameters

As already mentioned, the training of the ANN used only two input parameters, the density of the test specimens and the size class of the expanded clay. Additionally to the obvious proximity of the curves in Fig. 4, representing the results achieved by the two methodologies, the evaluation metrics "R-squared" (R^2) and the mean absolute percentage error (MAPE) were applied to ascertain the adjustability of the predicted parameters to the reference obtained by the H-S method.

Analysing Fig. 4, it is clear the very good agreement of the macroscopic parameters forecasted by the ANN model fed by only two input parameters (density of the test specimens and size class of the expanded clay) with the original data. It is also possible to conclude that, due to the more pronounced variability of the airflow resistivity data, the adjustment of Fig. 4c) is not as good as the adjustment of the other two output parameters. Fig. 5 presents the evaluation metric MAPE for this adjustment.

From Fig. 5, it can be verified the almost perfect agreement of the open porosity predicted values to the reference (original) data. In what concerns the tortuosity (α_{inf}), the ANN model returned 5.92% of error, while the error for the airflow resistivity (σ) reached 19.27%, which may mean that, for this specific parameter, the use of only two input parameters may lead to obtaining results that are not as rigorous as those obtained for the other two. Nevertheless, as it can be observed in Fig. 6, there is an excellent reproduction of the reference results by the predicted values of the ANN model.

For the open porosity parameter, the coefficient of determination is almost perfect ($R^2 = 0.99$), and, for the remaining parameters a R^2 of 0.8

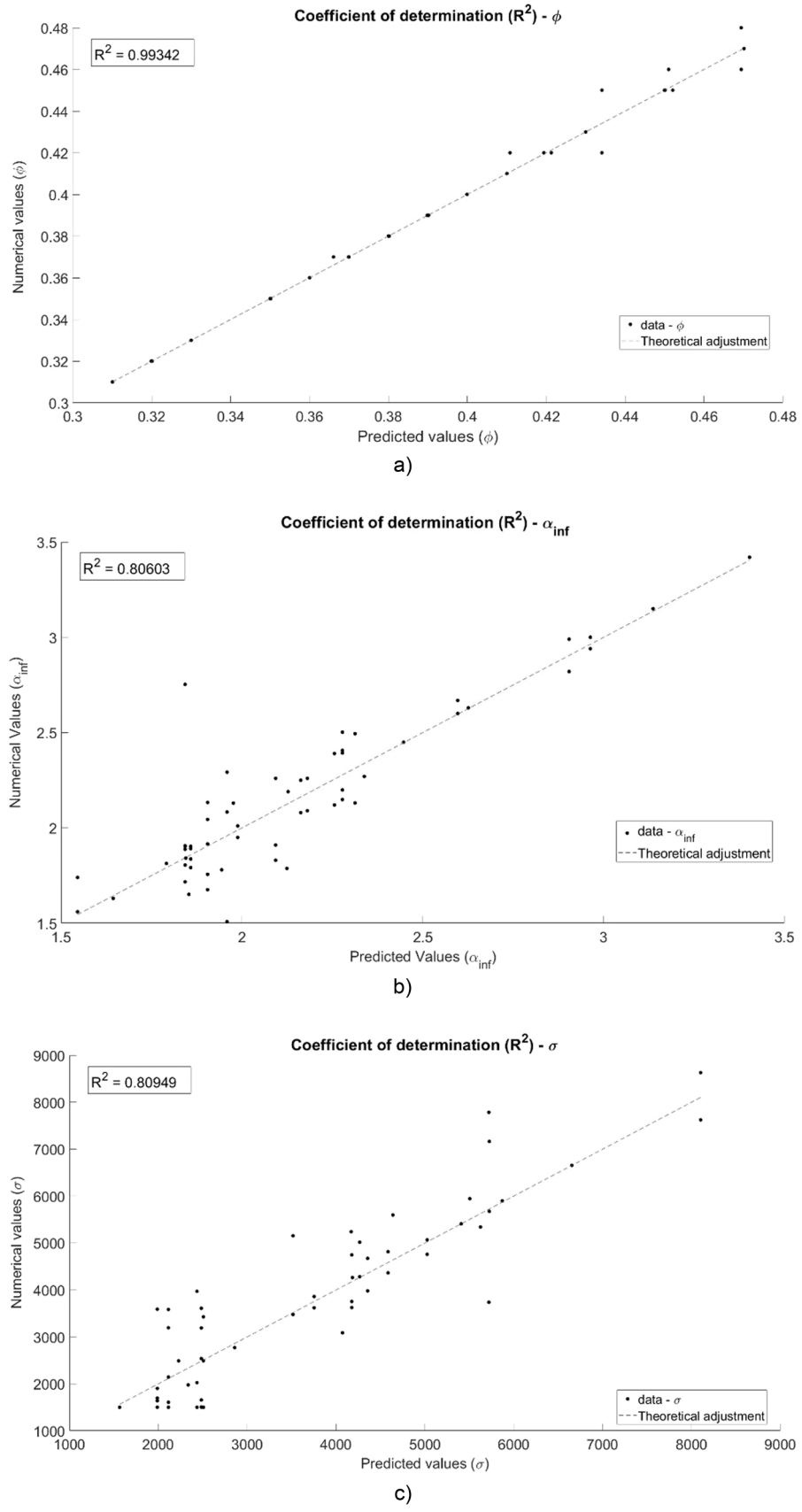

Fig. 6. Coefficient of determination (R^2) for a) open porosity - ϕ; b) Tortuosity - α_{inf}; c) Airflow resistivity - σ.

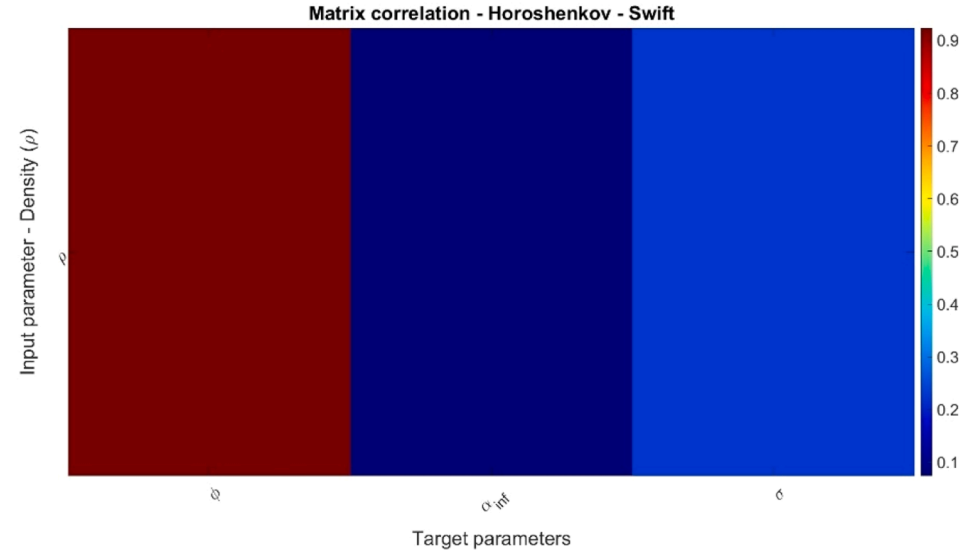

a)

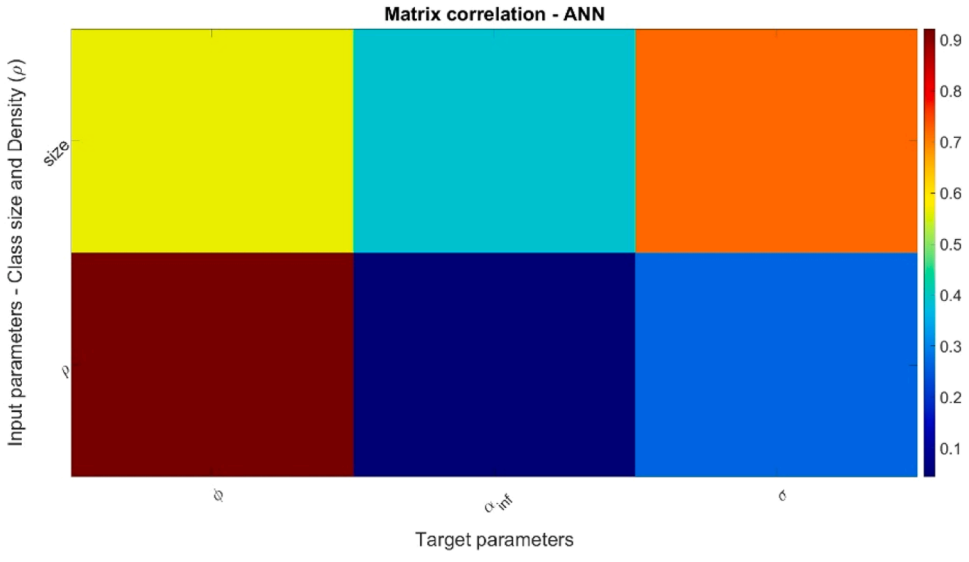

b)

Fig. 7. Correlation matrix between input and output parameters for both methodologies: a) Horoshenkov-swift; b) ANN model.

still indicates that approximately 80% of the variability in the data is explained by the ANN model, suggesting a strong relationship between the input and output variables.

5.2. Correlation between input and output parameters (original data and predicted scenarios)

An analysis to determine the relation between the input and output parameters was conducted during this study, and a comparison is presented in the heatmap of Fig. 7. Fig. 7.a) only considers the density of the test specimens.

Comparing the matrices, it is clear that the open porosity is greatly influenced by density with a 0.9 positive relation (in both methodologies), meaning that as the input parameter increases, the output parameter tends to increase proportionally. The matrices also indicate a very poor (<0.1) and low/moderate (0.3) influence of the density on the tortuosity and airflow resistivity, respectively. The similarity between the results of the two methods supports the coherence of the ANN model, suggesting that the results achieved by the ANN model are accurate and correct (nevertheless, it must be kept in mind that correlation matrices only try to correlate the variables linearly). The class size parameter, only evaluated in the ANN model correlation study, indicates a moderate influence of this parameter on the open porosity (0.55), a low/moderate influence on the tortuosity (0.4), and a significant influence on the airflow resistivity (0.7).

5.3. Determination of the absorption coefficient (α)

After the prediction of the macroscopic parameters by the ANN model, a calculation of the absorption coefficient (α) considering these parameters was conducted, and a comparison with the direct estimation using Horoshenkov-Swift method with the original data was performed. Two examples of absorption curves for the frequency range of 100–2000 Hz are presented in Fig. 8, illustrating scenarios taken from

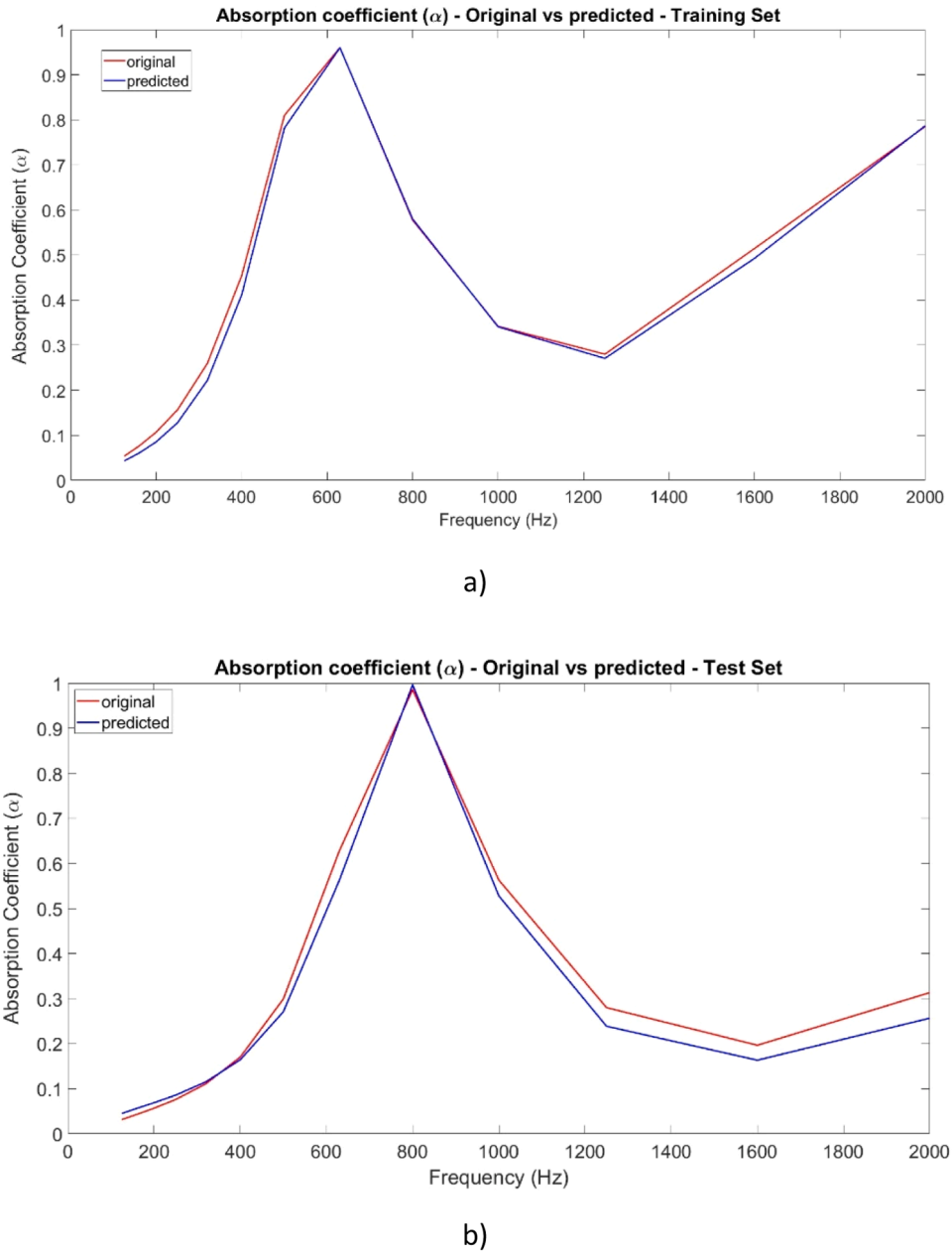

Fig. 8. Comparison examples of the absorption coefficient (α) calculated from the macroscopic parameters obtained by both methods: a) Training Set; b) Test Set.

the training (a) and test (b) data, sets that were used in the ANN training process.

From the analysis of Fig. 8, it can be concluded that the results of the absorption coefficient calculated from the macroscopic parameters obtained by the ANN model and the absorption coefficient obtained using the original data are very similar, which once again demonstrates the accuracy and reliability of the ANN model.

Fig. 9 presents six examples of the validation data set, an independent database that was not used in the training process of the ANN and that demonstrate unequivocally the performance capacity of the ANN.

From the analysis of the six examples of the Fig. 9, it can be verified the very good agreement between the absorption coefficient calculated from the original data and the one obtained from the macroscopic parameters predicted by the ANN. Fig. 10 presents the reproduction of the reference (original) results by the predicted values of the ANN model of the absorption coefficient parameter, for the same frequency range (100–2000 Hz).

The R-squared (R^2) of all datasets (training, test, and validation) demonstrate that there is a very good adjustment between the original and the ANN predicted values of the absorption coefficient. This means that the absorption coefficient calculated from the ANN model explains 92% of the variance of the same parameter calculated from the Horoshenkov-Swift methodology. It also means that the ANN model fits the training dataset well. In the presence of new, unseen data, the R-squared of 0.87 of the validation dataset, demonstrate the capacity of the ANN model to generalize competently and consistently in the presence of data not used during training.

5.4. *Determination of the relative importance of the input parameters*

The relative importance of the input variables in the ANN model was studied in MATLAB. The analysis focused on the determination of the contribution of individual input variables (grain size and density) to the overall predictive capability of the ANN model. To achieve this

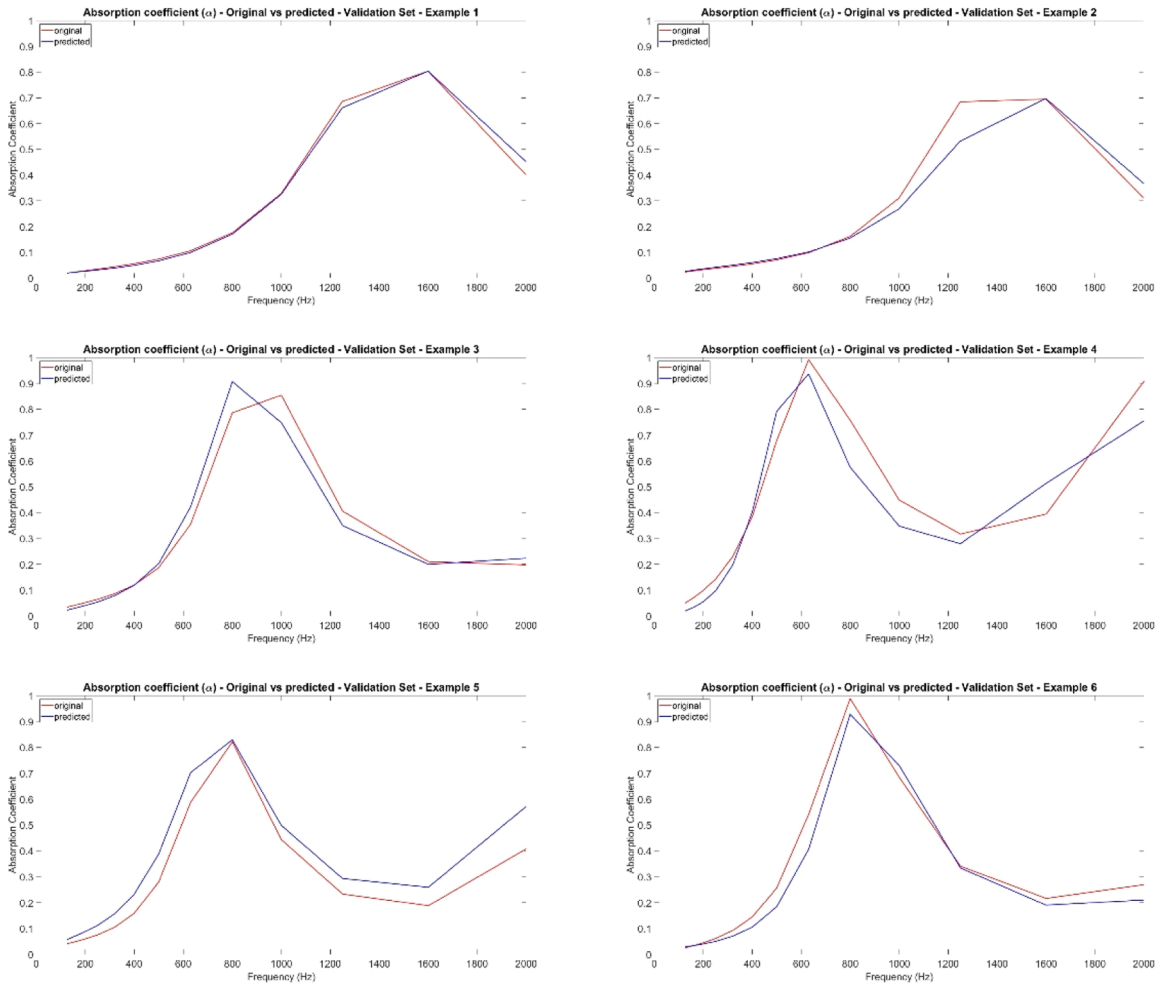

Fig. 9. Comparison examples of the absorption coefficient (α) calculated from the macroscopic parameters obtained by both methods: Validation Set.

objective, the weights from between the input and first hidden layer and between the last hidden and output layers were extracted from each neural network and computed, considering the absolute values of the weights of the mentioned relevant layers.

Specifically, for each input variable, the MATLAB code iteratively evaluated its importance by considering the cumulative contribution of absolute weights in the hidden layer and scales it by the absolute weights in the output layer, and, finally, to facilitate a direct comparison of the impact of each input parameter, the results were normalized to ensure that they collectively sum to 100%.

The relative importance (*RI*) of each input variable is calculated using the expression (9):

$$RI(\%) = \frac{\sum\left(\frac{|W1(:,n)|}{\sum|W1|}\right)}{\sum\left(\left(\frac{|W1(:,n)|}{\sum|W1|}\right)\times|W2(:,1)|\right)} \tag{9}$$

where n is the index of the input variable, $W1(:,n)$ represents the weights of the n *-th* input variable in the input-hidden layer, $W1$ represents all weights in the input-hidden layer, and $W2(:,1)$ represents the weights of the output variable of interest in the hidden-output layer.

The bar plots presented in Fig. 11 illustrate the varying degrees of influence that the input variables exert on the prediction of each material property considered in the study.

From the analysis of Fig. 11, it can be concluded that the grain size parameter is the most influential parameter in predicting open porosity (ϕ) and tortuosity (α_{inf}), with a relative importance of 58.02% and 59.17%, respectively. In the case of the airflow resistivity (σ), the results show that the most significant input parameter is the density, with a relative importance of 54.08%. However, a global analysis allows us to conclude that there is not a very pronounced difference in the relative influences of each input parameter, which means that both parameters have a similar importance in determining the output parameters.

It is important to highlight that, if we analyse simultaneously the graphs of Figs. 7 and 11, the results appear to be contradictory. According to Fig. 7, the most influential parameter in predicting open porosity is the density of the test specimen. Fig. 11 says otherwise. However, it is imperative to consider the substantial difference that exists both in the calculation of the correlation matrix and the relative importance, and the phase in which both methodologies are applied in any given research. The correlation matrix is usually applied at an early stage of a given study, aiming to determine a possible linear correlation (positive or negative) between variables. It is used to simplify the machine learning model, removing variables that are irrelevant to the system. The calculation of the relative importance is carried out through a detailed analysis of the weighted contributions of the first hidden layer and output layer of the neural network, after the network found non-linear relations between variables, thus providing a more flexible and accurate representation.

6. Conclusions

In this study, an artificial neural network model based only on two parameters that are simple and quick to obtain (size class of the

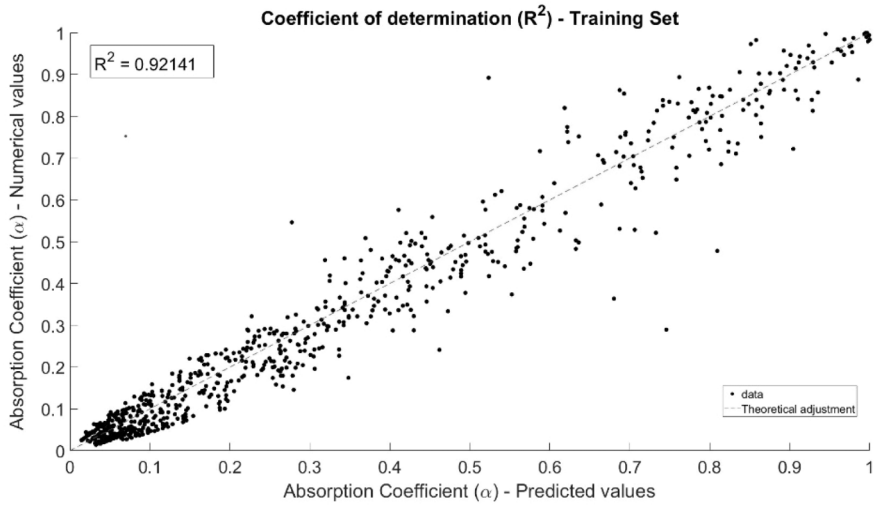

a)

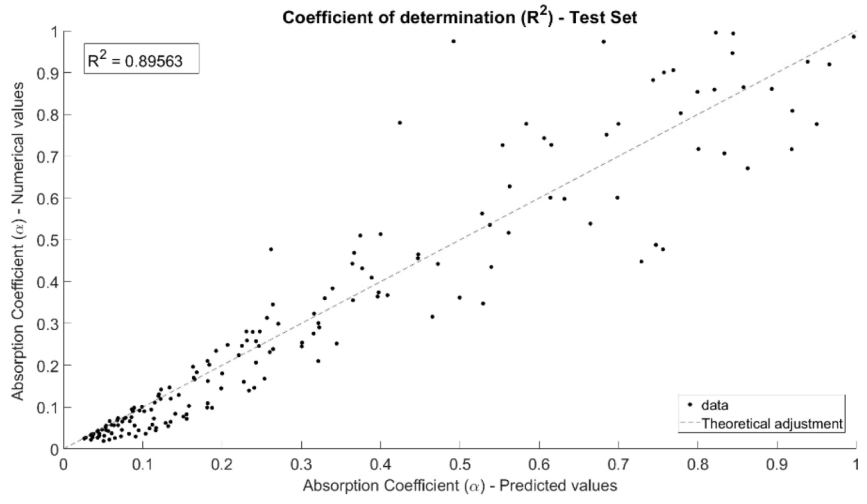

b)

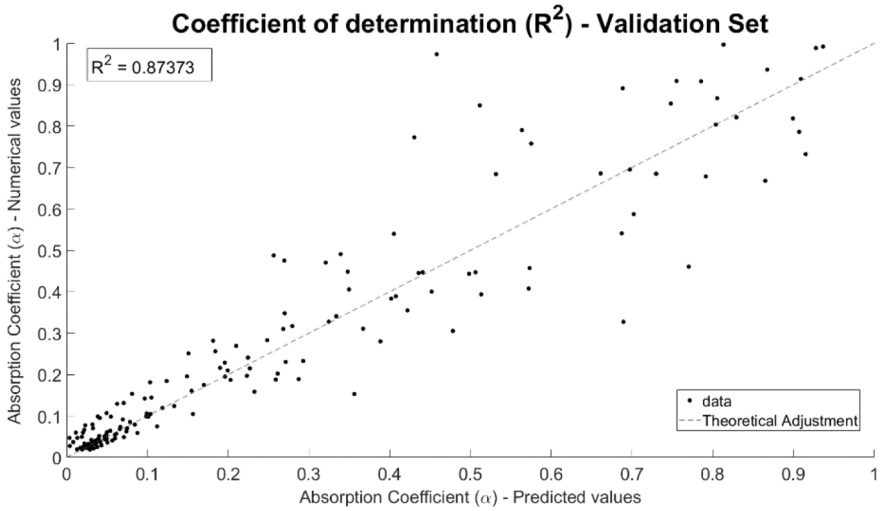

c)

Fig. 10. Coefficient of determination (R^2) of the absorption coefficient (α) for: a) Training Set; b) Test Set; c) Validation Set.

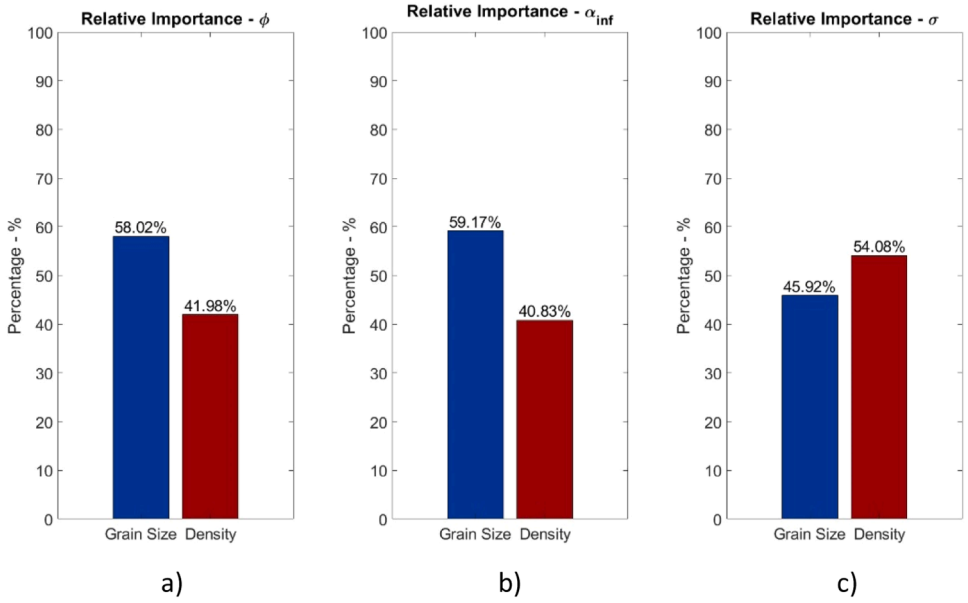

Fig. 11. Relative importance of the input parameters on each of the output parameters: a) Open porosity (ϕ); b) Tortuosity (α_{inf}); c) Airflow resistivity (σ).

expanded clay and density of the test specimens) was developed to predict, in a first phase, the macroscopic properties (open porosity, tortuosity and airflow resistivity) and finally the sound absorption coefficient (α) of these materials.

The results of the macroscopic parameters prediction indicate a good agreement with the results obtained through the more traditional inversion method, reinforced by the high similarity visible in the overlapping of the curves predicted by the ANN model and the Horoshenkov-Swift methodology, and by the R^2 of 0.99 for the open porosity and of 0.8 for the tortuosity and airflow resistivity. The mean absolute percentage error (MAPE) also indicate that this methodology is promising, despite the error of about 20% in the prediction of the airflow resistivity, which indicates that this specific parameter requires a substantially larger database (or more input parameters) to reduce this error.

The absorption coefficient results derived from the macroscopic parameters predicted by the ANN model closely match those obtained through the Horoshenkov-Swift method. This reaffirms the precision and dependability of the ANN model. The R-squared values for all datasets (training, test, and validation) indicate a highly effective alignment between the original and predicted absorption coefficient values. It was demonstrated that the absorption coefficient computed by the ANN model accounts for 92% of the variability observed in the same parameter calculated using the Horoshenkov-Swift methodology for the training dataset, and 89% for the test dataset. Additionally, it signifies the robust fit of the ANN model to the training and test datasets. Notably, the R-squared value of 0.87 for the validation dataset underscore the model's ability to generalize effectively and consistently when confronted with new, unseen data not utilized during the training phase.

The grain size parameter was identified as the most influential in predicting open porosity and tortuosity, while density is more significant for airflow resistivity.

The results of this study demonstrate the efficacy of the ANN approach in predicting macroscopic properties and sound absorption coefficients of porous concrete mixtures using only easy and simple to obtain input parameters: grain size of the expanded clay and density of the test specimens.

These results also show that ANN models provide an effective and simpler alternative to traditional methods when relevant datasets are available, making it a valuable tool for optimizing porous concrete formulations for specific acoustic requirements, and can be considered as viable, reliable and promising alternatives to the traditional approach.

Funding

This work was partly financed by FCT / MCTES through national funds (PIDDAC) under the R&D Unit Institute for Sustainability and Innovation in Structural Engineering (ISISE), under reference UIDB / 04029/2020 (doi.org/10.54499/UIDB/04029/2020), and under the Associate Laboratory Advanced Production and Intelligent Systems ARISE under reference LA/P/0112/2020.

This work is financed by national funds through FCT - Foundation for Science and Technology, under grant agreement 2022.12096.BD attributed to the 1st author.

CRediT authorship contribution statement

Luís Cortesão Godinho:Writing – review & editing, Supervision, Investigation, Conceptualization. Fernando G. Branco:Writing – review & editing, Supervision. Paulo da Venda Oliveira:Writing – review & editing, Supervision. Luís Pereira:Writing – review & editing, Writing – original draft, Methodology, Investigation.

Declaration of Competing Interest

The authors declare that they have no known competing financial interests or personal relationships that could have appeared to influence the work reported in this paper.

Data Availability

Data will be made available on request.

References

[1] M. Kurpińska, L. Kułak, T. Miruszewski, M. Byczuk, Application of artificial neural networks to predict insulation properties of lightweight concrete, Appl. Sci. vol. 11 (22) (Nov. 2021), https://doi.org/10.3390/app112210544.

[2] F. Asdrubali, K.V. Horoshenkov, The acoustic properties of expanded clay granulates, Build. Acoust. vol. 9 (2) (2002) 85–98, https://doi.org/10.1260/135101002760164553.

[3] J.-H. Tay, W.-K. Yip, Sludge ash as lightweight concrete material, J. Environ. Eng. vol. 115 (1) (1989) 56–64.

[4] K.V. Horoshenkov, M.J. Swift, The effect of consolidation on the acoustic properties of loose rubber granulates, Appl. Acoust. vol. 62 (6) (2001) 665–690, https://doi.org/10.1016/S0003-682X(00)00069-4.
[5] Y. Zaetang, A. Wongsa, V. Sata, P. Chindaprasirt, Use of lightweight aggregates in pervious concrete, Constr. Build. Mater. vol. 48 (2013) 585–591, https://doi.org/10.1016/j.conbuildmat.2013.07.077.
[6] M. Vašina, D.C. Hughes, K.V. Horoshenkov, L. Lapčík, The acoustical properties of consolidated expanded clay granulates, Appl. Acoust. vol. 67 (8) (2006) 787–796, https://doi.org/10.1016/j.apacoust.2005.08.003.
[7] K. Horoshenkov, M. Swift, Acoustic granular materials with pore size distribution close to log-normal, J. Acoust. Soc. Am. vol. 111 (5) (2002) 2378, https://doi.org/10.1121/1.4809157.
[8] M.A. Nielsen, Neural Networks and Deep Learning, vol. 25, Determination press, San Francisco, CA, USA, 2015.
[9] International Organization for Standardization, ISO 10534-2, Acoustics-Determination of Sound Absorption Coefficient and Impedance in Impedance Tubes. 2001. [Online]. Available: ⟨http://www.iso.org/iso/iso_catalogue/catalogue_tc/catalogue_detail.htm?csnumber=18603⟩.
[10] M. Pereira, J. Carbajo, L. Godinho, P. Amado-Mendes, D. Mateus, J. Ramis, Acoustic behavior of porous concrete. Characterization by experimental and inversion methods, –e202, Mater. De. Constr. vol. 69 (336) (2019) e202, https://doi.org/10.3989/mc.2019.03619.
[11] K.V. Horoshenkov, M.J. Swift, The acoustic properties of granular materials with pore size distribution close to log-normal, J. Acoust. Soc. Am. vol. 110 (5) (2001) 2371–2378.
[12] O. Umnova, K. Attenborough, K.M. Li, Cell model calculations of dynamic drag parameters in packings of spheres, J. Acoust. Soc. Am. vol. 107 (6) (2000) 3113–3119, https://doi.org/10.1121/1.429340.
[13] P. Bonfiglio, F. Pompoli, Comparison of different inversion techniques for determining physical parameters of porous media, ICA 2007 (2007) 1–6.
[14] J.F. Allard, Y. van, New empirical equations for sound propagation in rigid frame fibrous materials, J. Acoust. Soc. Am. vol. 91 (6) (1992) 3346–3353, https://doi.org/10.1121/1.402824.
[15] S.C. Jong, D.E.L. Ong, E. Oh, State-of-the-art review of geotechnical-driven artificial intelligence techniques in underground soil-structure interaction, Tunn. Undergr. Space Technol. vol. 113 (April) (2021), https://doi.org/10.1016/j.tust.2021.103946.
[16] W. Zhang, H. Li, Y. Li, H. Liu, Y. Chen, X. Ding, Application of deep learning algorithms in geotechnical engineering: a short critical review, Artif. Intell. Rev. vol. 54 (8) (2021) 5633–5673, https://doi.org/10.1007/s10462-021-09967-1.
[17] A. Szenicer, et al., Seismic savanna: machine learning for classifying wildlife and behaviours using ground-based vibration field recordings, Remote Sens Ecol. Conserv. vol. 8 (2) (2022) 236–250, https://doi.org/10.1002/rse2.242.
[18] M.W. Gardner, S.R. Dorling, Artificial neural networks (the multilayer perceptron) - a review of applications in the atmospheric sciences, Atmos. Environ. vol. 32 (14–15) (1998) 2627–2636, https://doi.org/10.1016/S1352-2310(97)00447-0.
[19] S.A. Kalogirou, Artificial neural networks in renewable energy systems applications: a review, Renew. Sustain. Energy Rev. vol. 5 (4) (2000) 373–401, https://doi.org/10.1016/S1364-0321(01)00006-5.
[20] Z. Zhang, K. Friedrich, Artificial neural networks applied to polymer composites: a review, Compos Sci. Technol. vol. 63 (14) (2003) 2029–2044, https://doi.org/10.1016/S0266-3538(03)00106-4.
[21] M.R.G. Meireles, P.E.M. Almeida, M.G. Simões, A comprehensive review for industrial applicability of artificial neural networks, IEEE Trans. Ind. Electron. vol. 50 (3) (2003) 585–601, https://doi.org/10.1109/TIE.2003.812470.
[22] P.J. Lisboa, A.F.G. Taktak, The use of artificial neural networks in decision support in cancer: a systematic review, Neural Netw. vol. 19 (4) (2006) 408–415, https://doi.org/10.1016/j.neunet.2005.10.007.
[23] Z. Waszczyszyn, Artificial neural networks in civil engineering: another five years of research in Poland, Comput. Assist. Mech. Eng. Sci. vol. 18 (3) (2011) 131–146.
[24] A.R. Bunawan, E. Momeni, D.J. Armaghani, K. Nissa binti Mat Said, A.S.A. Rashid, Experimental and intelligent techniques to estimate bearing capacity of cohesive soft soils reinforced with soil-cement columns, Measurement vol. 124 (November 2016) (2018) 529–538, https://doi.org/10.1016/j.measurement.2018.04.057.
[25] A. Baghbani, T. Choudhury, S. Costa, J. Reiner, Application of artificial intelligence in geotechnical engineering: a state-of-the-art review, Earth Sci. Rev. vol. 228 (2022) 103991, https://doi.org/10.1016/j.earscirev.2022.103991.
[26] O. Bello, J. Holzmann, T. Yaqoob, C. Teodoriu, Application of artificial intelligence methods in drilling system design and operations: a review of the state of the art, J. Artif. Intell. Soft Comput. Res. vol. 5 (2) (2015) 121–139, https://doi.org/10.1515/jaiscr-2015-0024.
[27] I.H. Sarker, Machine learning: algorithms, real-world applications and research directions, SN Comput. Sci. 2 (2021) 160.
[28] J.A. Flores, Focus on Artificial Neural Networks, Nova Science Publishers, 2021.
[29] L. Pereira, L. Godinho, F.G. Branco, Predicting unconfined compression strength and split tensile strength of soil-cement via artificial neural networks, Geomech. Eng. vol. 33 (6) (2023) 611–624, https://doi.org/10.12989/gae.2023.33.6.611.
[30] W. Mao, L. Hei, Y. Yang, Advances on the acoustic emission testing for monitoring of granular soils, Measurement vol. 185 (2021) 110110, https://doi.org/10.1016/j.measurement.2021.110110.
[31] H.Lo Lee, J.S. Kim, C.H. Hong, D.K. Cho, Ensemble learning approach for the prediction of quantitative rock damage using various acoustic emission parameters, Appl. Sci. vol. 11 (9) (2021) 4008, https://doi.org/10.3390/app11094008.
[32] L. Deng, A. Smith, N. Dixon, H. Yuan, Machine learning prediction of landslide deformation behaviour using acoustic emission and rainfall measurements, Eng. Geol. vol. 293 (8) (2021) 2959–2974, https://doi.org/10.1016/j.enggeo.2021.106315.
[33] P. Narloch, A. Hassanat, A.S. Tarawneh, H. Anysz, J. Kotowski, K. Almohammadi, Predicting compressive strength of cement-stabilized rammed earth based on SEM images using computer vision and deep learning, Appl. Sci. vol. 9 (23) (2019) 5131, https://doi.org/10.3390/app9235131.
[34] X. Shi, Q. Liu, L. Xiujuan, Application of SVM in predicting the strength of cement stabilized soil, Appl. Mech. Mater. vol. 160 (2012) 313–317, https://doi.org/10.4028/www.scientific.net/AMM.160.313.
[35] S. Suman, M. Mahamaya, S.K. Das, Prediction of maximum dry density and unconfined compressive strength of cement stabilised soil using artificial intelligence techniques, Int. J. Geosynth. Ground Eng. vol. 2 (2) (2016) 1–11, https://doi.org/10.1007/s40891-016-0051-9.
[36] Y. Liu, M. Li, P. Su, B. Ma, Z. You, Porosity prediction of granular materials through discrete element method and back propagation Neural Network algorithm, Appl. Sci. (Switz.) vol. 10 (5) (2020) 1693, https://doi.org/10.3390/app10051693.
[37] K.M. Graczyk, M. Matyka, Predicting porosity, permeability, and tortuosity of porous media from images by deep learning, Sci. Rep. vol. 10 (1) (2020) 1–11, https://doi.org/10.1038/s41598-020-78415-x.
[38] B. Boukhatem, R. Rebouh, A. Zidol, M. Chekired, A. Tagnit-Hamou, An intelligent hybrid system for predicting the tortuosity of the pore system of fly ash concrete, Constr. Build. Mater. vol. 205 (2019) 274–284, https://doi.org/10.1016/j.conbuildmat.2019.02.005.
[39] T. Lähivaara, L. Kärkkäinen, J.M.J. Huttunen, J.S. Hesthaven, Deep convolutional neural networks for estimating porous material parameters with ultrasound tomography, J. Acoust. Soc. Am. vol. 143 (2) (2018) 1148–1158, https://doi.org/10.1121/1.5024341.
[40] J.H. Jeon, S.S. Yang, Y.J. Kang, Estimation of sound absorption coefficient of layered fibrous material using artificial neural networks, Appl. Acoust. vol. 169 (2020) 107476, https://doi.org/10.1016/j.apacoust.2020.107476.
[41] S. Tola, J. Tinoco, J.C. Matos, E. Obrien, Scour detection with monitoring methods and machine learning algorithms—a critical review, Appl. Sci. vol. 13 (3) (2023) 1661, https://doi.org/10.3390/app13031661.
[42] J. Tinoco, A. Gomes Correia, P. Cortez, D.G. Toll, Data-driven model for stability condition prediction of soil embankments based on visual data features, J. Comput. Civ. Eng. vol. 32 (4) (2018) 4018027, https://doi.org/10.1061/(asce)cp.1943-5487.0000770.